Application of thermal atomic layer deposited Al_2O_3 in c-Si solar cells

Yue He (何 悦)[1], Yanan Dou (窦亚楠)[1,2*], and Junhao Chu (褚君浩)[2]**

[1]*Suntech Power Co., Ltd., Shanghai 201114, China*

[2]*Shanghai Institute of Technical Physics, Chinese Academy of Sciences, Shanghai 200083, China*

[*]*Corresponding author: yndou@mail.sitp.ac.cn;* [**]*corresponding author: jhchu@mail.sitp.ac.cn*

Received May 7, 2012; accepted June 25, 2012; posted online October 26, 2012

Thermal atomic layer deposited (ALD) Al_2O_3 films are applied at the front and rear sides of PERC-type c-Si solar cells. At the front side, Al_2O_3/SiN_x as a double-layer antireflection coating reduces the reflection loss, and at the rear side, Al_2O_3 film as the passivation layer decreases the surface recombination velocity and enhances the internal reflectance at near-infrared (NIR) band together with SiN_x layer. Due to the improvement in the reflectance combined with a decrease of the surface recombination velocity, the PERC solar cells show an improved J_{sc} by 0.2 mA/cm^2 compared with the full-area back surface field cell.

OCIS codes: 250.0250, 310.0310.

doi: 10.3788/COL201210.S22501.

There are many ways to improve the efficiency of the current industrial standard c-Si solar cells based on screen-print technology, e.g., reducing the photo loss and carrier recombination loss[1]. In current standard full-area back surface field (BSF) c-Si solar cells based on screen-print technology, SiN_x film is deposited by plasma enhanced chemical vapor deposition (PECVD) on the textured front side as the passivation dielectric layer as well as antireflection coating and BSF formed during co-firing following the Al paste printed on the rear side. Theoretical calculation showed that double layer and multi-layer antireflection coating reduced the photo loss at the surface[2,3]. Many materials have been investigated to replace the mono-layer SiN_x film, such as SiO_2/TiO_2, MgF_2/CeO_2, SiN_xO_y/SiN_x, and graded index SiO_xN_y[4–7]. Moreover, the rear of solar cells should be passivated by a suitable dielectric layer instead of the whole side Si-Al alloy BSF to increase infrared (IR) inter-reflection and reduce the recombination velocity.

Thin film of aluminum oxide (Al_2O_3) deposited by plasma-assisted and thermal atomic layer deposition provided almost-perfect surface passivation for p-type Si[8,9]. Meanwhile, the refractive index of ~1.7 and no significant absorption in the visible part of the solar spectrum, Al_2O_3 is very suitable to be as the reflection coating for solar cell, especially as the front layer of a double-layer stack with SiN_x together. Thus, an advanced structure of PERC-type solar cell with Ag screen-printed contacts at the front and local BSF at the rear as demonstrated in Fig. 1 is very potentially applied industrially in the future. In this letter, thermal atomic layer deposited (ALD) Al_2O_3 films were applied in the c-Si solar cells as antireflection coating at the front and as passivation layer at the rear side.

125×125 (mm) solar cells were fabricated on 200-μm 1–3-Ω cm p-type Cz-Si wafers. The process flow is shown in Fig. 2. After cleaning procedure including a KOH-based damage etching, phosphorus diffusion using $POCl_3$ as precursor gas resulted in a sheet resistance of 55 Ω/□ for a single side. The phosphosilicate glass (PSG) and p-n junction at the edge were removed by HF and/or HNO_3 etching. Afterwards, the samples were merged to deposit a SiN_x layer at the front by an in-line PECVD system. The deposition temperature was around 480 °C resulting in a refractive index of 2.05 and a thickness of 80 nm. Followed, 10–30-nm amorphous Al_2O_3 films were simultaneously deposited at both sides of c-Si solar cell by thermal atomic layer deposition using $Al(CH_3)_3$ dosing and H_2O at a substrate temperature of 200 °C. The total reflectance

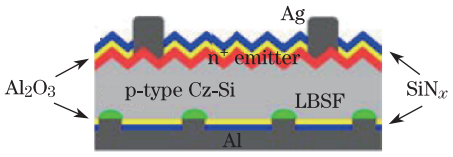

Fig. 1. Schematic of the PERC solar cells with Al_2O_3/SiN_x anti-reflection coating at the front and rear contacts with Al_2O_3/SiN_x (or Al_2O_3) rear passivation layer.

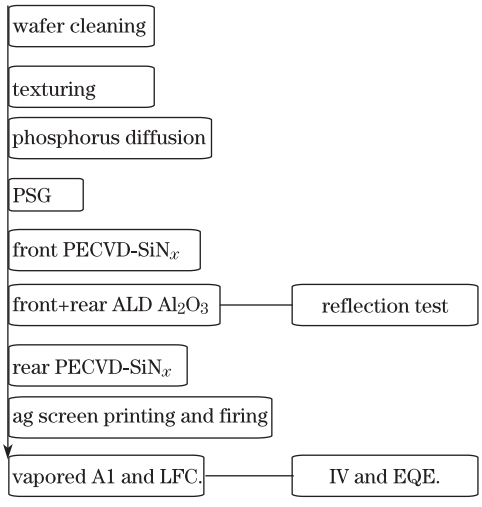

Fig. 2. (Color online) Schematic of the solar cell process flows and tests. The red boxes show the additional steps for the PERC cells compared with the reference process for standard solar cells and the green boxes show the characterization tests.

with wavelength from 300 to 1 100 nm was then characterized by Cary 5 000 UV-VIS-NIR spectrophotometer with an integrating sphere. Another 80-nm SiN_x film was deposited at the rear in order to protect the thin Al_2O_3 films. Using the screen printing process Ag front contacts show a finger width of 90 μm. At last, 2-μm-thick aluminum film was vapored at the rear and local point contact was formed by laser firing using a 1 064-nm laser. The point diameter was about 30 μm and the point pitch was set to be 0.5 mm. A local BSF is formed during laser fired contact[10]. At last, IV and external quantum efficiency (EQE) were characterized. In this process, we used vapored aluminum instead of Al paste because the Al paste was easy to penetrate into SiNx layer and destroy the Al_2O_3 films during firing.

Figure 3 presents the surface reflectance of 80-nm SiN_x and 10–30-nm Al_2O_3/SiN_x stacks on the textured Si wafers. The solar spectra at AM1.5 divided into three waveband regions are also shown in Fig. 3. In the ultraviolet (UV) band, the reflectance of stacks is higher than that of monolayer SiN_x, except for the 30-nm Al_2O_3 film below 350 nm. The increase of thickness of Al_2O_3 films makes the lowest peak red-shift. In the dominated solar spectra of visible and near-infrared (NIR) waveband, the double-layer coatings show their excellent reflection performance and almost reduce the reflectance to zero compared to the single SiN_x layer. The weighted reflectance[2] related to the short current is a more useful and simple parameter to characterize the reflectance performance. It is defined as

$$\overline{R} = \int_{\lambda_{\min}}^{\lambda_{\max}} F(\lambda)R(\lambda)Q(\lambda)\mathrm{d}\lambda \Big/ \int_{\lambda_{\min}}^{\lambda_{\max}} F(\lambda)Q(\lambda)\mathrm{d}\lambda, \quad (1)$$

where $F(\lambda)$ is the photon flux of the solar spectrum

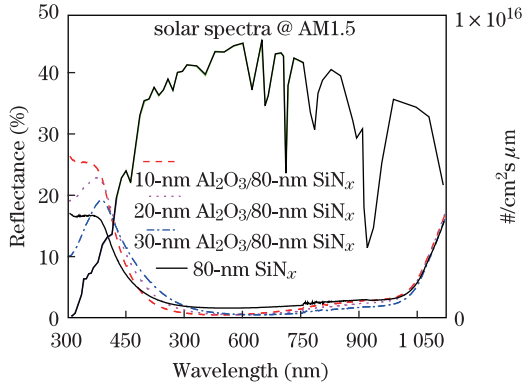

Fig. 3. (Color online) Experimental reflectance of mono-layer SiN_x and 10–30-nm $Al_2O_3/SiNx$ stacks on the textured Si surface. The solar spectra at AM1.5 are also shown, with violent, green, and IR lines representing the UV, visible and NIR regions.

Table 1. Weighted Reflectance of SiN_x and Al_2O_3/SiN_x Stacks

Structure	Weighted Ref.
80-nm-SiN_x	2.93
10-nm Al_2O_3/80-nm SiNx	2.52
20-nm Al_2O_3/80-nm SiNx	2.61
30-nm Al_2O_3/80-nm SiNx	2.58

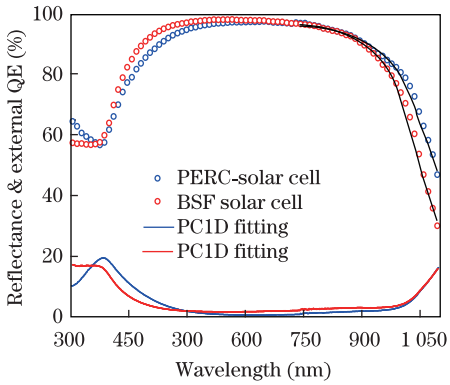

Fig. 4. (Color online) Comparison of measured EQE and reflectance between PERC (with 25-nm Al_2O_3 film) solar cell and a standard screen-print full-area Al-BSF reference cell. In the long wavelength region, the EQE was simulated using the software PC1D, from which the surface recombination velocity and internal reflectance were extracted.

and $Q(\lambda)$ is the internal quantum efficiency of PERC solar cell. The weighted reflectances of all these samples are calculated and the results are shown in Table 1, with $\lambda_{\min}$=300 nm and $\lambda_{\max}$=1 100 nm. All over the solar spectra, the Al_2O_3/SiN_x stack reduces the reflectance from 2.9% to 2.5%. The improvement of 14% reflectance can increase the absolute efficiency of solar cell by ~0.1%. However, the efficiency of this cell suffers from the low fill factor (FF) due to the poor contact at the front by inline IV test, because the Ag paste is difficult to completely penetrate into the Al_2O_3/SiN_x stack in a normal co-firing process.

For a detailed analysis PERC and Al-BSF solar cells were characterized by measuring their EQE using OL series 750 automated spectroradiometric measurement system, as shown in Fig. 4. In this PERC solar cell, the thickness of Al_2O_3 film is 25 nm. In the UV band and long wavelength region, we can clearly see the strong improvement of the reflectance and EQE due to the anti-reflection coating and dielectric rear surface passivation stack. By using the software PC1D, the EQE was simulated in the IR region. It results in the rear recombination velocity S_{rear} of 370 cm/s and the internal reflectance R_{b} of 95%. In contrast, the referenced full-area Al-BSF cell shows the S_{rear} of 500 cm/s and R_{b} of 75%. Due to the increase in the internal reflectance combined with an increase of the surface passivation quality, the PERC solar cells show an improved the short circuit current J_{sc} by 0.2 mA/cm^2 compared with the full-area BSF reference cell. The improvement of the surface passivation is not very obvious may be due to that high-temperature firing destroyed the interface structure of Al_2O_3/Si substrate and increases the defects states originating from dangling bonds.

In conclusion, industrial PERC-type solar cells with thermal ALD Al_2O_3 films applied are fabricated. The Al_2O_3/SiN_x stacks do usefully reduce the surface reflectance in most of the wavelength region and enhance the internal reflectance in long wavelength region. Meanwhile, the Al_2O_3 dielectric layer improves the surface passivation. As a result, an increase of J_{sc} by 0.2 mA/cm^2 compared with the full-area BSF reference cell is obtained.

This work was supported by the Foundation for Innovative Research Groups of China (Nos. 60821092, U1037604), Innovation Project of Shanghai Institute of Technical Physics (No. QZY51), and Shanghai Rising-Star Program (No. 11QB1406800).

References

1. T. Saga, NPG Asia Mater. **2,** 96 (2010).
2. J. Zhao and M. A. Green, IEEE Trans. Electr. Dev. **38,** 1925 (1991).
3. W. Wang and H. Hao, Chin. Opt. Lett. **8,** 35 (2010).
4. C. Martinet, V. Paillard, A. Gagnaire, and J. Joseph, J. Non-Cryst. Solids **216,** 77 (1997).
5. S. E. Lee, S. W. Choi, and J. Yi, Thin Solid Films **276,** 208 (2000).
6. J. Dupuis, J.-F. Lelièvre. E. Fourmond, V. Mong-The Yen, O. Nichiporuk, N. Le Quang, and M. Lemiti, in *Proceedings of* 24th *EUPVSEC* 1636 (2009).
7. M. Lipiński, A. Kaminski, J.-F. Lelièvre, M. Lemiti, E. Fourmond, and P. Zięa, Phys. Stat. Sol. (c) **4,** 1566 (2007).
8. B. Hoex, S. B. S. Heil, E. Langereis, M. C. M. van de Sanden, and W. M. M. Kessels, Appl. Phys. Lett. **89,** 042112 (2006).
9. G. Dingemans, R. Seguin, P. Engelhart M. C. M. van de Sanden, and W. M. M. Kessels, Phys. Status Solidi-RRL **4,** 10 (2010).
10. E. Schneiderlöchner, R. Preu, R. Lüdemann, and S. W. Glunz, Progress in Photovoltaics **10,** 29 (2002).